International Journal of
INTELLIGENT SYSTEMS AND APPLICATIONS IN ENGINEERING
ISSN:2147-6799 www.ijisae.org Original Research Paper

A Comparative Study of Support Vector Machine and Maximum Likelihood Classification to Extract Land Cover of Wasit Governorate-Iraq

Noora B. Shwayyea Al-Aayedi*[1], Mutasim I. Malik[2] and Hazim B. Taher[3]

Submitted: 28/01/2023 **Accepted:** 01/04/2023

Abstract: In order to effectively describe land cover, scientists, academics, and researchers developed machine learning classification algorithms. According to studies, these classification techniques perform better than more tried-and-true conventional techniques. The primary aim of this project is to determine the most effective strategy for categorizing land cover in order to retrieve data from Wasit. The Maximum Likelihood Classifier (MLC), which is based on the neighborhood function, and the Support Vector Machine (SVM), which is based on the ideal hyper-plane function, are two supervised classification techniques that are contrasted using Sentinel-2 data. Four land cover classes have been chosen for this optimization. Four spatial layers of the research region were surveyed with the aim of collecting and providing field-based training samples. The error matrix and kappa statistics have been used to evaluate the accuracy of each classifier. Results demonstrated that SVM performs superior to MLC. SVM and MLC have overall accuracies of 99.79 and 99.60%, respectively, and kappa coefficients of 0.997 and 0.994.

Keywords: land cover, accuracy assessment, support vector machine, maximum likelihood classification, and kappa coefficients.

Introduction: Both land cover and land use. For all living things, land is a basic necessity, and its usefulness depends on the purpose for which it is used. It is typically defined as an area of the earth's surface where living things carry out their daily activity. It serves as a multi-resource foundation for humanity by providing food, clothing, shelter, forestry, fruits, and vegetables. According to Chiemelu and Onwumere (2013), the land in that area is a major factor in the economics and prosperity of the nation. Generally, people confuse land usage and land cover and think that they are the reverse of one another.

Role of GIS and remote sensing in land cover: Land cover has an immediate impact on the environment's quality, the water cycle of the area, and the variety of living organisms. Significant data regarding the land cover may now be easily observed and instantly captured thanks to remote sensing technologies (Abdi, 2020; Ngo et al., 2020; Cui,2019). Outstanding applications that help to understand the complex dynamics of the environment have been generated as a result of the development of remote sensing (RS) and geographic information system (GIS) technology. In this context, spatial analytical methods like land cover change detection, land cover classification, and land cover mapping play a key role in supplying crucial data on land cover at the local and global levels (Gupta and Srivastava, 2010). Land cover data may be analyzed and mapped efficiently with the correct remote sensing and GIS correlation tools. Programs utilizing satellite data for remote sensing aspire to accurately classify land cover (Wulder et al., 2018; Hutt et al., 2016).

Classifiers that are non-parametric and parametric. The most broadly used words in classification techniques are parametric and non-parametric classifiers. The data distribution for each individual class .The data distribution for each individual class is taken into account by parametric classifiers to be normal. Maximum Likelihood Classification is the most extensively used, standard, and widely used parametric classifier (MLC). Decision surfaces are produced by this classifier using the data's mean and covariance (Srivastava et al., 2012). The normal distribution of the data is not the foundation of a non-parametric classifier, and little is assumed about the data's statistical significance. The support vector machine, which combines multiple machine learning techniques and is used for classification, is one of the non-parametric classifiers (Varma et al., 2016). In 1971, Vapnik and Chervonenkis developed the SVM theory as a binary classification technique. In 2000, Vapnik developed the

[1]*Department of Physics, College of Science, University of Sumer ;*
[2]*Department of Physics, College of Science, University of Wasit*
[3] *Republic of Iraq, Ministry of Higher Education and Scientific Research*
** E-mail of the corresponding author: noorabalbool@gmail.com*

SVM further. SVM, a machine learning approach based on artificial intelligence, has been applied in several remote sensing applications (Varma et al., 2016; Taati et al., 2015; Ustuner et al., 2015).

Current Issues and Difficulties. The support vector machine, which uses a variety of machine learning approaches and is one of the non-parametric classifiers, is used for classification (Varma et al., 2016). As a binary classification technique, Vapnik and Chervonenkis developed the SVM theory in 1971. In 2000, Vapnik made additional SVM improvements. SVM, an AI-based machine learning technique, has been applied in several remote sensing applications (Varma et al.,2016; Taati et al.,2015; Ustuner et al., 2015) For instance, satellite remote sensing provides precise geographic information about the land cover of any location worldwide in real-time (Puletti et al.,2018;Olmanson and Bauer, 2017).Researchers and scientists looked at a range of picture classification approaches to extract and map information regarding land cover (Thanh and Kappas, 2018). Due to the placement of multiple satellites in orbit, access to data is no longer a problem; the real challenge is in the interpretation of the data. The main difficulty is sorting these satellite data into categories and removing important information without sacrificing its accuracy. Since high dimension picture data also contains information on the geographical distribution of items on the earth's surface and a variety of spectral properties, conventional classification algorithms have limits when it comes to the interpretation of substantial volumes of high dimension image data. A comprehensive sample set and prior knowledge are both challenging to get and occasionally unattainable. Traditional approaches are unable to address these issues because they lack the capacity for self-learning. Ngo et al., 2020; Abdi, 2020; Cui, 2019). These restrictions must be overcome because machine learning approaches self-learn via the process. The ideal method for identifying land cover has been investigated in a number of studies, but additional comparative study is required to establish which approach is most effective. By contrasting three of these machine learning classifiers with the conventional classification approach, Nitze et al (2012). Because they self-learn during the process, machine learning techniques are essential for getting over these restrictions. There have been numerous studies done to find the best method for classifying land cover, however more comparative studies are required to figure out which strategy is best. In order to discriminate between several crop kinds, Nitze et al. (2012) contrasted three such machine learning classifiers with the traditional method. Data from Rapideye was used to enhance the SVM's performance (5m resolution). The SVM method's overall accuracy was 68.6%. Similar research was done by Nguyen and Kappas (2018) using data from the Sentinel-2 satellite (10 m resolution), comparing and analyzing the abilities of three classifiers: random, k-nearest neighbor, and support vector machine. The results of the classification show a decent overall accuracy of 90–95 percent.

SVM had the highest overall accuracy compared to the other classifiers. In the current work, two supervised classifiers—Support Vector Machine (SVM) and Maximum Likelihood Classifier—have been compared and evaluated (MLC).Sentinel-2 remote sensing satellite data are utilized to compare the wasit governorate's categorisation accuracy to choose the best method.

Materials and Methods.

Study area. Wasit Governorate has a population of roughly 1163700 and an area of approximately 17753 km^2, or 4% of Iraq's total area (437,072 km^2)[T. M. F. Al-Azzawi,2018]. It is situated between the following coordinates: Latitude: 32° 13' 60.00"N and Longitude: 46°17' 60.00"E in eastern Iraq or the southern section of the central area of Iraq. Through the Abramabad border crossing near Wasit, it has a land border with the Islamic Republic of Iran. The governorates of Diyala, Baghdad, Babil , Qadissiya , Thi-Qar and Missan are bordered by it internally. The Tigris River cuts through Wasit, where a belt of irrigated farmland extends to the northeast before giving place to a desert environment. In this study, the entire Wasit area is enclosed as shown in figure (1). Al-Kut, Al-Hai, Al-Na'maniya, Al-Suwayra, Aziziya, and Badrah are the six districts that make up the governorate of Wasit [R. I. M. Al-quraishi,2019].Iraqi city Al-Kut serves as Wasit Province's administrative center. It is situated 180 kilometers southeast of Iraq's capital city, Baghdad. It is situated 353 kilometers northeast of Dewania, 187 kilometers north of Nasiriya, and 191 kilometers northwest of Amara, 238 kilometers south of Diyala, 272 kilometers east of Babylon, 100 kilometers west of Iran. The study's 232 Km^2 total area is located between[D. S. Sha,2016]:**Longitude:**45° 49' 23.304" E and **Latitude:** 32° 30' 21.708"N.

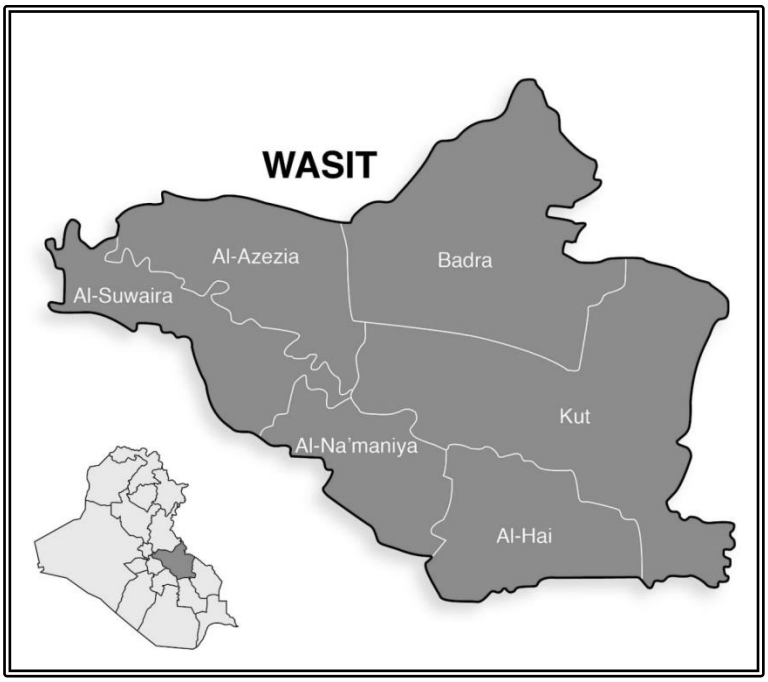

Fig. (1): Location of Wasit Governorate/ Iraq.

Table (1) displays the spectral and spatial ranges of these 10 bands.

Band	**Resolution**	**Central Wavelength**	**Description**
B1	60 m	443 nm	Ultra-Blue (Coastal and Aerosol)
B2	10 m	490 nm	Blue
B3	10 m	560 nm	Green
B4	10 m	665nm	Red Visible and Near Infrared (VNIR)
B5	20 m	705 nm	Visible and Near Infrared (VNIR)
B6	20 m	740 nm	Visible and Near Infrared (VNIR)
B7	20 m	783nm	Visible and Near Infrared (VNIR)
B8	10 m	842 nm	Visible and Near Infrared (VNIR)
B8a	20 m	865 nm	Short Wave Infrared (SWIR)
B9	60 m	940 nm	Short Wave Infrared (SWIR)
B10	60 m	1375 nm	Short Wave Infrared (SWIR)
B11	20 m	1610 nm	Short Wave Infrared (SWIR)
B12	20 m	2190 nm	Short Wave Infrared (SWIR)

Data sets. In this study, two images from the Sentinel-2 satellite from the same season (summer, Sep. 2020) were used to analyze the land use and land cover of Wasit Governorate. These images were chosen because they had no clouds and were not considerably affected by atmospheric scattering and absorption effects. Owing to the fact that the study region does not fit inside a single grid, two images from an MSI sensor with the reference codes T43SDR and T43RDQ were used in accordance with Sentinel-2's reference grid system. Both images' calendar dates were selected to reduce the seasonal effect. The optical, near-infrared, and short wave infrared bands were picked from the total of 10 bands in the Sentinel-2A dataset for picture classification. In the study, a selection of images based on the vector district border was taken into account to cut down on computation time.

Interpretation of satellite images. When the satellite image acquisition date is the same and the desired classes are approximated from the spectral signature, atmospheric corrections are often not needed for image classification, but they are crucial when one needs to do change detection (Chrysoulakis et.al.,2010). Vanonckelen et al. state that atmospheric corrections are required when using several photos at various temporal

levels (2013). Ortho-rectification, geometric, and atmospheric correction had previously been applied to the Sentinel-2A photos. The geo referencing of the imported Sentinel-2A imagery was checked against a vector data layer for the area before being imported into ENVI 5.3 Imagine software. The output image file was prepared for use once the layers were layered. In this study, two images from the Sentinel-2 satellite from the same season (summer, 2020) were used to analyze the land use and land cover of Wasit Governorate. These images were selected because they were not significantly impacted by atmospheric scattering and absorption effects and were free of clouds. table (2) show the original image, which has a size of 10980*10980 pixels and a spatial resolution of roughly (60, 20, 10) meters, and the clipped image of a part of Wasit governorate, which has a size of 6189*6155 pixels and a resolution of (10m). The clipped image was created by extracting the region of interest (part of Wasit Governorate) from the original image using a clipping tool, which helps to reduce the amount of data and improve the efficiency of the analysis. The clipped image has a higher resolution (10m) compared to the original image, which can provide more detailed information of the study area.

Table (2): The sets of scenes downloaded from USGS site for Sentinel-2

No.	Name	Date	Time	Orbit no.
1	S2B_MSIL1C_20200925T073649_N0209_R092_T38SNA_20200925T090135.SAFE	2020/9/25	07:36:49	92
2	S2A_MSIL1C_20200920T073621_N0209_R092_T38SNB_20200920T085340.SAFE	2020/9/20	07:36:21	92

The Sentinel-2 product type utilized in this study is S2 level-1C, which corresponds to the Top of Atmosphere (TOA) reflectance in cartographic geometry. The granules, also known as tiles, for this level are 100 km^2 ortho-images in the UTM/WGS84 projection. Each 100 x 100 Km^2 tile is around 500 MB in size.

The pre-processing and classification process used to produce the results for Sentinel-2 images is depicted in the flowchart below in figure (2):

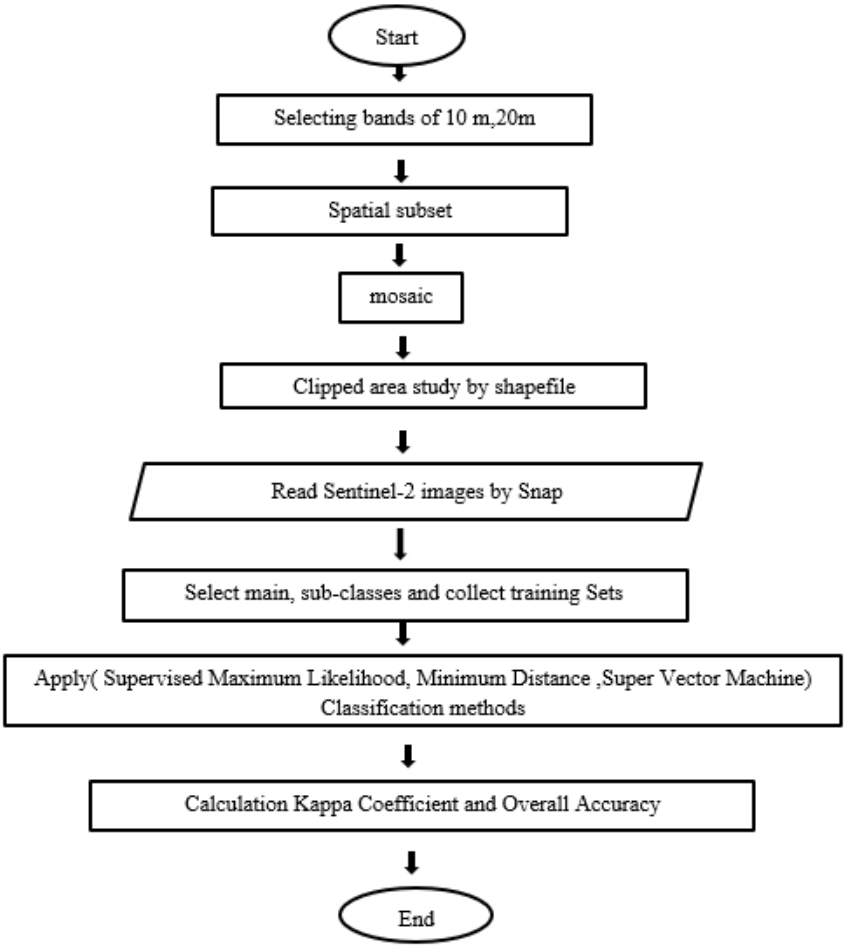

Fig. (2): Flowchart Setinel-2 MSI images classification process.

Maximum likelihood classification (MLC). The MLC technique assesses statistical information such as covariance and variances of the chosen class signatures before giving values to the unknown pixels from the represented class signature file. This strategy presupposes that the data distribution in multidimensional space is linear or normal and is based on the Bayes theorem of decision-making. Under the presumption of a linear distribution, a class is described using its covariance matrix and mean vector. One of these two elements is allotted to each pixel value. Statistical probabilities are computed for each class to determine the cell relevance to that class. Based on the previously stated weights, each pixel has been assigned to the land cover class to which it has the highest similarity (Srivastava et al., 2012) The following Bayesian equation (1) calculates the likelihood of an unknown value from a known class value (Otukei and Blaschke (2010).

$$g_i(x) = Ln\left(p(w_i)\right) - \frac{1}{2}\ln(p)\,|\Sigma i| - \frac{1}{2}(x - m_i)^2 \sum_i^{-1} (x - m_i) \ldots\ldots (1)$$

Where:

$g_i(x)$: function of discriminant.

Ln (x) : natural logarithm for dimensional information x.

$p(w_i)$: probability that the class w_i find in image.

$|\Sigma i|$: Specification for the information covariance matrix in class w_i.

$\sum_i^{-1}$: inverse of a covariance matrix.

w_i : image classes mean vector.

Support vector machine (SVM) classification. SVM converts non-separable decision boundaries from an input dataset into separable decision boundaries of feature space or higher multi-dimensional space using user-supplied kernel functions. SVMs are supervised learning algorithms that are non-parametric and have a statistical basis. Each pair of classes is separated by an OSH that the algorithm discovers. Using training data from the study area, an OSH was created. Finding the OSH among the other separating hyper-planes is the main goal of SVM. This is accomplished by resolving a quadratic programming and Lagrange multiplier optimization problem (Szuster et al., 2011). Vladimir Vapnik developed the Support Vector Machine (SVM), a learning tool that attempts to construct decision functions in the input space by using the idea of structural risk reduction.

SVM also includes creating one or more hyper planes to partition the various classes. According to Vapnik and Cortes, an ideal hyper plane is a linear decision function with the largest margin between the vectors of the two classes.

when the instances are perfectly isolated from one another and the hyper plan is the furthest away from the closest instance, we consider the best hyper plan, which can be defined as:

$$W^T x + b = 0\,, x \in R^d \quad \ldots\ldots\ldots\ldots\ldots\ldots (2)$$

Samples close to the hyperplan's edges are referred to as "support vectors." They are used to determine which hyperplan should be chosen because the best hyperplan divides this set of vectors [R. G. Congalton, 1991].

SVM is widely used as a linear decision function when the data may be divided. Nonetheless, we assume that the data are linearly non-separable for the purposes of this study. We must therefore propose a nonlinear function with nonnegative variables I that can map the data in a high-dimensional feature space where they can be linearly separated in order to map the data in a space where they can be linearly separated. The vector W that minimizes the functional cost can be used to locate the best hyperplan in a nonlinear space.

$$\Phi(\mathbf{W}, \boldsymbol{\xi}) = \frac{1}{2}\|W\|^2 + C\sum_{i=1}^{i} \xi_i \ldots\ldots\ldots\ldots\ldots\ldots (3)$$

Where C is a predetermined value used to regulate the degree of regularization and ξ is a slack variable [R. G. Congalton, 1991].

Classification system. The range and spatial (10m) resolution of the image were taken into consideration when designing the following system (see Fig.2 and Table3).

Table (3): The classes colors that adopted in the classified images.

Class no.	Main classes	Color	Sub-classes	Color
1	Urban		Urban	
2	plants		Agricultural land	
3	water		Tigris River	
			Marshland	
4	Soil		Sandy Soil	
			Dry soil	
			Salty Soil	

Accuracy Assessment. The classifiers' accuracy is assessed with the use of reference datasets.

The accuracy is assessed using an error matrix or confusion matrix. By contrasting it with the validation data, of the categorization outcome. A well-known parameter in accuracy evaluation, the kappa co-efficient was calculated using the equation:

$$\textbf{Overall Accuracy} = \frac{\textbf{Total no. of correct classified pixels}}{\textbf{Total no. of pixels}} \times 100\% \quad \textbf{.... (4)}$$

Whereas overall accuracy is the proportion of accurate pixels among all the pixels in the same category, overall accuracy is the ratio of properly classified pixels to all the reference pixels. Instead of class-specific accuracy, the user's accuracy evaluates overall correctness. The accuracy of the producer and the user's category measures are in fact related to error of omission and error of commission, respectively (Gupta and Sirivasstava, 2010).

The Kappa coefficient is "one of the easiest statistics to know the validity of the classification using the error matrix," according to[S. N. Sivanandam and etl. 2007], and it is calculated using the matrix table that contains all the classified and reference data. By calculating the classification's affinity with the reference data and comparing the results, the quantity of mistakes is determined.

$$\boldsymbol{K} = \frac{\boldsymbol{n}\sum_{i=1}^{p} x_{ii} - \sum_{i=1}^{p}(x_{i+} \times x_{+i})}{\boldsymbol{n^2} - \sum_{i=1}^{p}(x_{i+} \times x_{+i})} \quad \textbf{..... (5)}$$

Where,

n = total number of training pixels

p = number of classes

$\sum x_{ii}$ = total number elements of confusion matrix

$\sum x_{i+}$ = sum of row i

$\sum x_{+i}$ = sum of column i

Results and Discussion:

MLC results. The MLC approach was used to create land cover classification maps using Sentinel-2 images with a 10-m resolution. To determine the impact of training dataset size, four different training sample sizes were used. These datasets display various overall accuracy percentages (Fig. 3).

The overall accuracy of MLC reduces as the number of training samples size increases. Due to an increase in the quantity of training pixels and the use of likelihood pixels rather than learning algorithms to construct decision boundaries in MLC.

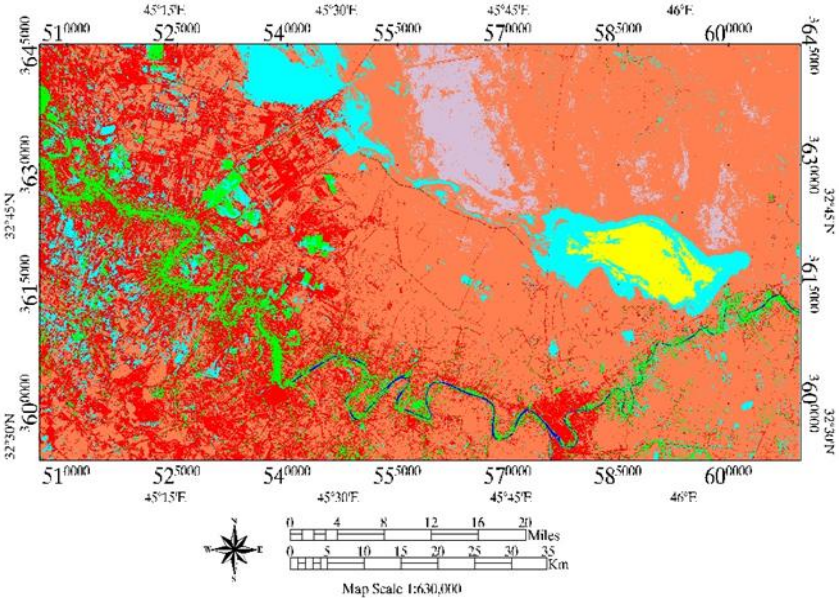

Fig. (3): Classification results for S2-images with resolution(10 m) for apart of Wasit 2020 using maximum likelihood classifier.

Table (4): Statistics of sub-classes for areas measured in units of (Km²).by ML

Class Name	Class color	Area (km^2) for 10 m	Area in %
Urban Cover	Red	1,154.2 Km²	21.20%
Agricultural land	Green	329 Km²	6%
Tigris River	Blue	15.6 Km²	0.20%
Salty Soil	Yellow	95.6 Km²	1.70%
Marshland	Cyan	525.1 Km²	9.60%
Sandy Soil	Thistle	233.2 Km²	4.30%
Dry soil	Coral	3,066.7 Km²	56.50%

SVM results. For SVM classification, the same datasets—Sentinel-2 and four different training data sizes—were also utilized. More training datasets increase SVM's overall accuracy, but sample size has little of an effect (Fig. 4).

SVM is a machine learning technique, and as the size of the training sample grows, the algorithm has more data to find support vectors that extend farther margins, leading to the lowest generalization error possible. The maximum overall accuracy of the SVM algorithm is 99.79%.

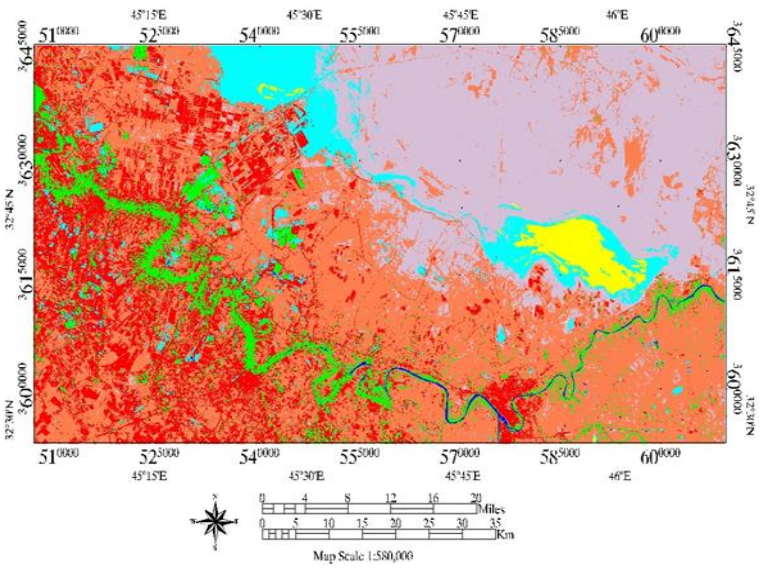

Fig. (4): Classification results for S2-images with resolution(10 m) for apart of Wasit 2020 using SVM classifier.

Table (5): Statistics of sub-classes for areas measured in units of (Km²).by SVM.

Class Name	Class color	Area (km^2) for 10 m	10 m
Urban Cover	Red	894.4 Km²	16.50%
Agricultural land	Green	329 Km²	6%
Tigris River	Blue	17.2 Km²	0.30%
Salty Soil	Yellow	91.5 Km²	1.60%
Marshland	Cyan	378.5 Km²	6.90%
Sandy Soil	Thistle	1,469.5 Km²	27.10%
Dry soil	Coral	2,241.8 Km²	41.30%

Table(6) Overall Accuracy and Kappa statistics of MLC and SVM in tabular form

Classification	Maximum likelihood	SVM
Overall Accuracy	%99.60	%99.79
Kappa Coefficient	0.994	0.997

Comparison of MLC and SVM. The classification techniques with the highest overall accuracy scores were chosen for comparison. how many training .There are varying sample sizes for each classification algorithm, such as 100 for MLC and 400 for SVM. To evaluate the accuracy of each classification method's performance in separating land cover classes, error matrices for each method were created. The distinction between the two approaches is clear:

The size of the training samples has no bearing on the accuracy of the SVM method's land cover classification; the same results can be obtained with either a small or large number of training examples. In contrast to it, accuracy of land cover categorization in MLC approach is significantly dependent upon the size of the training sample Moreover, compared to MLC, SVM method displays a more spatially coherent map. With the SVM approach, built-up areas are also better defined, and accuracy values reflect these. The accuracy of the open/bare class increased by 5% when utilizing the SVM technique. Water accuracy remained unchanged while the planted/cultivated class experienced a modest 2% gain (Table 5). Although both classifiers have produced results with acceptable accuracy and reliability, SVM is generally considered to be superior to MLC. Szuster et al. (2011) for Thailand reported a similar outcome for this comparison. Using ASTER data with a spatial resolution of 15 m, he was able to successfully achieve accuracy of 94.15 percent for SVM and 93.9 percent for MLC. Its accuracy has increased to 95.20 percent for SVM in the current work because to the adoption of superior spatial and spectral resolutions. This comparison demonstrates the superiority of higher spatial resolution differences. As was predicted, the MLC approach gave a lower total accuracy of 88.80%. MLC effectively divides cultivated or planted land from bare or open terrain, but it performs less well when dealing with water and built-up areas. Just 30 of the 45 water pixels are accurately classified.

planted/cultivated pixels as water is applied. Similar to this, built-up pixels and open/bare land pixels are merged, and 76 of the 78 pixels are correctly classified using the MLC approach. The accuracy provided by the water cover class was the lowest overall, coming in at only 66.67%. For the other three classes—built-up area, planted/cultivated, and open/bare—the producer's accuracy was fair (97.44%, 93.33%, and 88.46%, respectively) Table 4. The SVM approach produced better results, with an overall accuracy of 95.20 percent. Also, this approach improved user accuracy for each category of land cover. It operates differently from the decision boundaries in MLC in terms of class separation and offers a sizable separating hyper-plane for each class. The highest increase was in built-up land, which increased from 80.00% using the MLC approach to 90.24% using the SVM methodology. Kappa measures. Comparing the two categorization methods' highest Kappa coefficients. It's interesting to see the water class's kappa coefficient.

The overall number of categorized pixels and the total number of correctly classified pixels are comparable in both methods (45 in SVM and 30 in MLC), however the fraction of incorrectly classified pixels is higher in MLC than in SVM. Hence, the categorization is 1 in both cases. The SVM method also exhibits exceptional accuracy for the other three groups. Built-up land cover sees an increase in kappa accuracy of 0.15 from 0.70 in MLC to 0.85 in SVM, 0.04 from 0.90 to 0.94 in SVM for planted/cultivated land cover, and 0.08 from 0.89 to 0.97 in SVM for bare/open land cover. Srivastava et al. (2012) report that SVM's Kappa accuracy is 0.74, higher than MLC's 0.71. The difference between this study's four bands (from Landsat TM) and this investigation's ten bands is negligible (Sentinel-2). Moreover, 236 out of 250 pixels were accurately identified using SVM and MLC. A value of zero indicates that the classification is no more accurate than random categorization, and the kappa coefficient ranges from -1 to 1. Values close to or equal to 1 indicate that classification is noticeably superior to random classification, whereas a value of -1 indicates that classification is inferior to random classification.

Conclusion and suggestion : The mapping of diverse land cover types presents a recurring problem for academics. The results show that a support vector machine classifier can classify land cover with a kappa coefficient of 0.93 and an overall accuracy of 95.20 percent, outperforming other classifiers when given medium scale pictures (10-m Sentinel-2). SVM also fared better at categorizing mixed groups than higher

dimensional data and the wasit governorate. The other equivalent approach makes use of a maximum likelihood classifier, which has a kappa coefficient of 0.84 and a total accuracy of 88.80%. SVM outperforms MLC for the spectral ranges and resolution of Sentinel-2A images, according to the evaluation of the classifiers' accuracy using example Sentinel-2A data. The results, however, might change if SVM is applied to datasets with different spectral ranges. Due of SVM's exceptional accuracy, hyper-spectral imageries are advised. The parameter and kernel affect SVM accuracy. Thus, it is possible to learn about the land cover by running a sensitivity analysis on a number of kernels.

Built-up areas can be further separated into dense, moderate, and low density zones to determine population density properly. The cultivated/agricultural land cover can also be further classified in order to glean detailed details on the kinds of crops grown in a particular region. High resolution satellites are recommended for classification since they meet a wide range of requirements and uses for urban and agricultural development, risk assessment, planning, and policy making.

Incompatible interests. The authors say they have no competing interests.

Reference:

[1] Abdi, A.M. 2020. Land cover and land use classification performance of machine learning algorithms in a boreal landscape using Sentinel-2 data. GIScience & Remote Sensing, 57: 1-20. (https://doi.org/10.1080/15481603.2019.1650447) .

[2] Brar, G.S. 2013. Detection of land use and land cover change with Remote sensing and GIS: A case study of Punjab Siwaliks. International Journal of Geomatics and Geosciences, 4: 296-304. (https:// www.semanticscholar.org/paper/Detection-of-landuse-and-land-cover-change-with-ABrar /1667abddcd5cb786cbb68543c26580f2d3555f20).

[3] Census. 2017. Provisional summary results of 6th population and housing census-2017. Pakistan bureau of statistics. (http://www.pbs.gov.pk/content/provisional-summary-results-6th-population-andhousing-census-2017-0).

[4] Chiemelu, N.E., Onwumere, V.O. 2013. Land information systems for efficient land administration and revenue generation: a case study of tans-amadi industrial layout. Port Harcourt, Nigeria, Journal of Information Engineering and Application, 3:13-23. (https://www.iiste.org/Journals/index.php/JIEA/article/view/8920) .

[5] Chrysoulakis, N., Abrams, M., Feidas, H., Arai, K. 2010. Comparison of atmospheric correction methods using ASTER data for the area of Crete, Greece. International Journal of Remote Sensing, 31: 6347-6385. (https://www.researchgate.net/publication/253497600).

[6] Cui, H.S. 2019. Sub-urban land classification using GF-2 images and support vector machine method. In:Proceedings of International Conference on Advances in Civil and Ecological Engineering Research, pp. 351 012028, Kaohsiung, Taiwan.(https://iopscience.iop.org/article/10.1088/1755-1315/351/1/012028/meta)

[7] Gupta, M., Srivastava, P.K. 2010. Integrating GIS and remote sensing for identification of groundwater potential zones in the hilly terrain of Pavagarh, Gujarat, India. Water International, 35: 233-245. (https://www.tandfonline.com/doi/full/10.1080/02508061003664419).

[8] Hütt, C., Koppe, W., Miao, Y., Bareth, G. 2016. Best accuracy land use/land cover (LULC) classification to derive crop types using multi-temporal, multisensor, and multi-polarization SAR satellite images.Remote Sensing, 8: 684. (https://doi.org/10.3390/rs8080684)

[9] Ngo, K.D., Lechner, A.M., Vu, T.T. 2020. Land cover mapping of the Mekong delta to support natural resource management with multi-temporal Sentinel-1A synthetic aperture radar imagery. Remote Sensing Applications: Society and Environment,17: 100272. (https://doi.org/10.1016/j.rsase.2019.100272)

[10] Nitze, I., Schulthess, U., Asche, H. 2012. Comparison of machine learning algorithms random forest, artificial neural network and support vector machine to maximum likelihood for supervised crop type classification. In: Proceedings of 4th GEOBIA, pp.35, Rio de Janeiro - Brazil. (https://www.researchgate.net/profile/Ingmar_Nitze/publication/275641579)

[11] Olmanson, L.G., Bauer, M.E. 2017. Land cover classification of the lake of the woods/rainy river Basin by object-based image analysis of Landsat and lidar data. Lake and Reservoir Management,33: 335-346. (https://doi.org/10.1080/10402381.2017.1373171)

[12] Otukei, J.R., Blaschke, T. 2010. Land cover change assessment using decision trees, support vector machines and maximum likelihood classification algorithms. International Journal of Applied Earth Observation and Geoinformation, 12: S27–S31. (https://doi.org/10.1016/j.jag.2009.11.002)

[13] Puletti, N., Chianucci, F., Castaldi, C. 2018. Use of Sentinel-2 for forest classification in Mediterranean environments. Annals of Silvicultural Research,42: 32-38. (http://dx.doi.org/10.12899/asr-1463)

[14] Riaz, O., Ghaffar, A., Butt, I. 2014. Modelling land use patterns of Lahore (Pakistan) using remote sensing and GIS. Global Journal of Science Frontier Research. Environment & Earth Science, 14: 24-30. (https://www.researchgate.net/profile/Omar_Riaz/publication/281741257)

[15] Sajjad, S.H., Batool, R., Qadri, S.T., Shirazi, S.A., Shakrullah, K. 2015. The long-term variability in minimum and maximum temperature trends and heat island of Lahore city, Pakistan. Science International, 27: 1321-1325. (https://www.researchgate.net/profile/Sm_Talha_Qadri/publication/280802787).

[16] Srivastava, P.K., Kiran, G., Gupta, M., Sharma, N., Prasad, K. 2012. A study on distribution of heavy metal contamination in the vegetables using GIS and analytical technique. International Journal of Ecology & Development, 21: 89-99. (http://www.ceserp.com/cp-jour/index.php/ijed/article/view/3936).

[17] Szuster, B.W., Chen, Q. Borger, M.A. 2011.comparison of classification techniques to support land cover and land use analysis in tropical coastal zones. Applied Geography, 31: 525-532. (https://doi.org/10.1016/j.apgeog.2010.11.007)

[18] Taati, A., Sarmadian, F., Mousavi, A., Pour, C.T.H., Shahir, A.H.E. 2015. Land use classification using support vector machine and maximum likelihood algorithms by Landsat 5 TM images. Walailak Journal of Science and Technology, 12: 681-687. (https://doi.nrct.go.th//ListDoi/listDetail?Resolve_DOI=10.14456/wjst.2015.33)

[19] Thanh N.P., Kappas, M. 2018. Comparison of random forest, k-nearest neighbor, and support vector machine classifiers for land cover classification using Sentinel-2 imagery. Sensors, 18:18. (https://doi.org/10.3390/s18010018).

[20] Ustuner, M., Sanli, F.B., Dixon, B. 2015. Application of support vector machines for landuse classification using high-resolution RapidEye images: a sensitivity analysis. European Journal of Remote Sensing, 48:403-422. (https://doi.org/10.5721/EuJRS20154823)

[21] Vanonckelen, S., Lhermitte, S., Rompaey, A.V. 2013.The effect of atmospheric and topographic correction methods on land cover classification accuracy. International Journal of Applied Earth Observation and Geoinformation, 24: 9-21. (https://doi.org/10.1016/j.jag.2013.02.003).

[22] Varma, M.K.S., Rao, N.K.K., Raju, K.K., Varma, G.P.S.2016. Pixel-based classification using support vector machine classifier. In: Proceedings of IEEE 6th International Conference on Advanced Computing, pp. 51-55, Bhimavaram, India (https://ieeexplore.ieee.org/abstract/document/7544809)

[23] Wulder, M.A., Coops, N.C., Roy, D.P., White, J.C., Hermosilla, T. 2018. Land cover 2.0. International Journal of Remote Sensing, 39: 4254-4284. (https://doi.org/10.1080/01431161.2018.1452075).

[24] T. M. F. Al-Azzawi and A. A. S. Al-Zirgany, "Change Detection for Some Land Cover Types of Wasit Province (Eastern Iraq) Using Remote Sensing and GIS Techniques for Years 1989," Indian J. Nat. Sci., vol. 9, no. 51, pp. 15359–15367, 2018.

[25] R. I. M. Al-quraishi, "Environmental Geochemistry of Wasit Governorate, Iraq," University of Baghdad, College of Science, Department of Geology, 2019.

[26] D. S. Sha, "Land Use And Land Cover Classification And Change Detection Using Naip Imagery From 2009 To 2014 : Table Rock Lake Region , Missouri," Geography, Geology and Planning, Missouri State University, 2016.

[27] R. G. Congalton, "A review of assessing the accuracy of classifications of remotely sensed data," Remote Sens. Environ., vol. 37, no. 1, pp. 35–46, 1991, doi: 10.1016/0034-4257(91)90048-B.

[28] S. N. Sivanandam, S. Sumathi, and S. N. Deepa, Introduction to fuzzy logic using MATLAB. Springer-Verlag Berlin Heidelberg, 2007.

[29] M. Sreelekha, "Accuracy Assessment of Supervised and Unsupervised Classification using NOAA Data in Andhra Pradesh Region," Int. J. Eng. Res., vol. 8, no. 12, pp. 60–64, 2019, doi: 10.17577/ijertv8is120065.